Proceedings of the 2007 IEEE/RSJ International
Conference on Intelligent Robots and Systems
San Diego, CA, USA, Oct 29 - Nov 2, 2007

High-speed 3D Image Acquisition Using Coded Structured Light Projection

Idaku Ishii, Kenkichi Yamamoto, Kensuke Doi, Tokuo Tsuji
Hiroshima University
1-4-1 Kagamiyama, Higashi-hiroshima, Hiroshima 739-8527, JAPAN
e-mail: iishii@robotics.hiroshima-u.ac.jp

Abstract— **In various application fields, high-speed cameras are used to analyze high-speed phenomena. Coded structured light projection methods have been proposed for acquiring three-dimensional images. Most of them are not suitable for measuring high-speed phenomena because the errors are caused when the measured objects move due to light projection of multiple patterns. In this paper, we propose a new coded structured light projection method that can select not only a temporal encoding but also a spatial encoding adaptively for obtaining three-dimensional images at a high-speed frame rate. We also develop an evaluation system that uses a DLP projector and an off-line high-speed video camera, and verify the effectiveness of the proposed method by showing the obtained three-dimensional shapes for moving objects.**

I. Introduction

In recent times, three-dimensional measurement technology has been used for various applications such as human modeling, industrial inspection, and cultural properties recording. Light sectioning method and coded structured light projection method are typical methods used to obtain three-dimensional shapes by projecting light information on objects and using this information for their measurement; further, three-dimensional capturing systems that can operate at 30 fps or more [1], [2] have already been developed following the improvements in integration technology in the last few years. Many high-speed video cameras can capture images at 1000 fps or more, and they have already been used for analyzing high-speed phenomenon. Nevertheless, in many fields, it is necessary to observe high-speed phenomena as three-dimensional shapes at a high-speed frame rate; however, most of the high-speed video cameras can only record high-speed phenomena as two-dimensional image sequences.

In this paper, we propose a spatio-temporal selection type coded structured light projection method for three-dimensional dynamic image acquisition at a high-speed frame rate. In fact, we evaluate our proposed algorithm by showing the experimental results of three-dimensional shapes obtained in the case of several moving objects; these shapes are captured at 1000 fps on a verification system comprising a DLP projector and an offline high-speed video camera.

II. Coded structured light projection method

Our proposed three-dimensional measurement method is based on the coded structured light projection method proposed by Posdamer et al [3]. In this section, we describe a basic principle of the coded structured light projection method and the related previous studies.

A. Basic principle

In the coded structured light projection method, zebra light patterns are projected in order to measure objects from a projector, as shown in Fig. 1; subsequently, a three-dimensional image is calculated from the projection images captured by a camera whose angle of view is different from that of the projector. The measurement space is divided into 2^n vertical pieces, when n is the number of zebra light patterns. We can then obtain n bit data at each pixel of the projection image, which corresponds to whether the light patterns are on or not. This n bit data is called a space code, and it shows a projection direction. Finally, we calculate the distance information at all pixels as an image using triangulation, based on the relationship between such a space code image and the measurement directions that are decided by pixel positions.

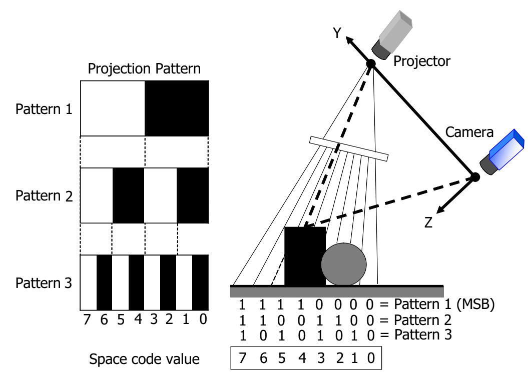

Fig. 1. Coded structured light projection method

B. Related works

Posdamer et al [3] used multiple black and white light patterns with a pure binary code, as shown in Fig.1. However, this might generate severe encoding errors even if there are only small noises, since the brightness boundaries of the multiple patterns are in the same positions. To solve this problem, Inokuchi et al [4] introduced gray code light pattern projections, which can minimize encoding errors with boundaries. Bergmann proposed an improved three-dimensional shape measurement method [5], which combines gray code pattern projection method and phase shift method, while the number of projection patterns increases. Caspi et al [6] proposed a color-type gray code pattern projection method that reduces the number of projection patterns.

These methods can obtain high-resolution three-dimensional images because distance information is calculated at every pixel, whereas noises are generated when the measured objects are moving because of multiple light patterns that are projected at different times.

Several three-dimensional measurement methods that use only one projection pattern are also proposed. Maruyama et al [7] introduced a light pattern with multiple slits of different lengths, whose encoding is based on the length of the slits. Durdle [8] proposed a measurement method based on a single light pattern that periodically arranges slits with three types of gray scale. These methods have a disadvantage that some ambiguity occurs in spatial encoding when there are pixels whose brightness are the same in its spatial neighborhood. To solve this ambiguity, several methods introduced color slit pattern projections using de Bruijn sequences as a robust coded pattern projection [9], [10]. These spatial encoding methods can measure the three-dimensional shapes of moving objects using only a single projection pattern; however their space resolution are not accurate as obtained with the methods that use multiple projection patterns.

III. Spatio-temporal Selection Type Coded Structured Light Projection Method

A. Concept

The coded structured light projection method based on multiple light patterns enables a highly accurate three-dimensional measurement for a static object, while the method using a single light pattern has robustness for a moving object as described in the previous section. In this paper, we propose a spatio-temporal selection type coded structured light projection method that attempts to combine the advantages of both measurements; high accuracy in the case of a static object and robustness in the case of a moving object.

Our proposed concept has the following features: (a) projection of multiple coded structured light patterns that enable both encoding along the time axis and encoding in the spatial neighborhood, (b) adaptive selection of encoding types in every local image region by calculating the image features those are dependent on the measured objects' motion. As a result, encoding along the time axis is selected in the region where there is no motion, while encoding in the spatial neighborhood is selected in the region where the brightness changes dynamically. The concept of the proposed method is shown as a figure in Fig. 2.

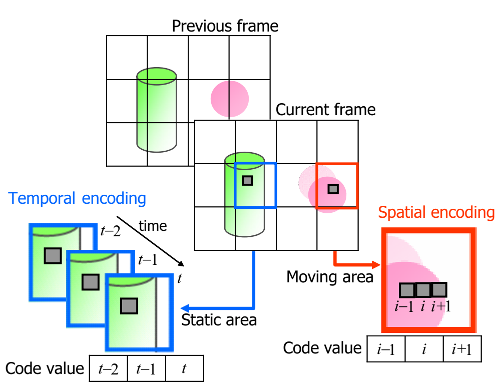

Fig. 2. Concept of our proposed method

B. Proposed coded structured light pattern

In our proposed method, a projected binary image for a coded structured light pattern is assumed to be the following equation:

$$I(x,y,t) = G\left(\left\lfloor \frac{x}{m} + t \right\rfloor \bmod n, y\right). \tag{1}$$

Here $I(x,y,t)$ represents the value of pixel (x,y) at a time t in the projected binary image. $\lfloor x \rfloor$ means the greatest integer less than or equal to x. The space code is assumed to be n bits, and m is the unit width of a light pattern in the x direction. $G(k,y)$ represents n types of one-dimensional gray code pattern $(0 \le k \le n-1)$ in the y direction, which can minimize encoding errors on code boundaries. $G(k,y)$ is expressed as

$$G(k,y) = \left\lfloor \frac{y \times 2^k}{I_y} + \frac{1}{2} \right\rfloor \bmod 2. \tag{2}$$

Here, the size of $I(x,y,t)$ is set as $I_x \times I_y$ pixels.

The coded pattern defined by Eq. (1) has a spatially periodic branched pattern based on the gray code, and shifts in the x direction over time. These features in the coded pattern enable spatio-temporal selection type encoding that can select not only encoding along the time axis but also encoding in the spatial neighborhood.

As an example of the coded patterns, Fig. 3 shows the patterns when the number of bits of the space codes is set as $n = 8$. In the figure, four coded patterns at time $t = 0$, 1, 2, and 3 are shown, and the numbers $k(=0,\cdots,7)$ at the bottom in each image indicate that the one-dimensional pattern in the y direction is set to $G(k,y)$. It can be seen that the space code can be generated only by using spatial neighborhood information, because eight gray code patterns

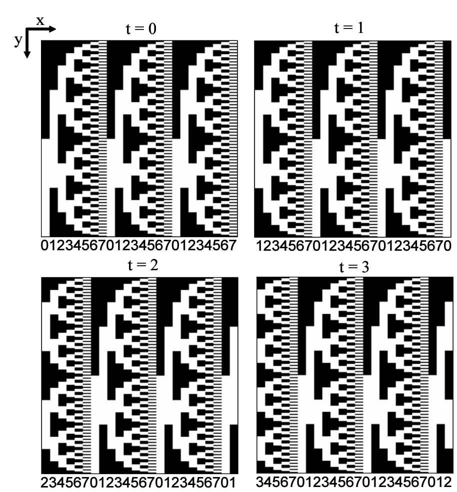

Fig. 3. Coded structured light patterns for spatio-temporal selection

– $G(0,y),\cdots,G(7,y)$ – are periodically arranged in a single image. The projected pattern also shifts to the left after a certain period of time, and the gray code pattern on the same pixel changes $G(0,y),G(1,y),G(2,y),\cdots$ every unit time. In this manner, we can obtain a space code at each pixel along the time axis.

C. Spatio-temporal selection type encoding algorithm

1) Calibration between a projection pattern and a captured image: The shifting light pattern is projected using a projector to measure objects, and the projection results are then captured as an image by a camera whose angle of view is different from that of the projector. For calculating space codes by using such a captured image, the type of gray code patterns expressed in Eq. (1) that is projected at each pixel on the captured image must be identified.

Fig. 4 shows the spatial relationship between the xy coordinate system of a projector and the $\xi\eta$ coordinate system of a camera. We assume that the x axis and ξ axis are parallel for light patterns projected from the projector and captured images by the camera.

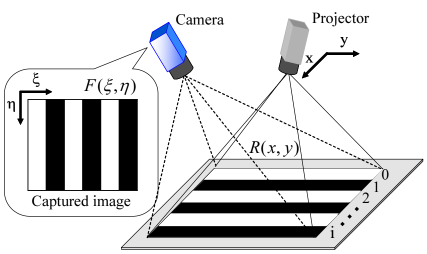

Fig. 4. Spatial relationship between a projector and a camera

Here a region that corresponds to a gray code pattern $G(k,y)$ is referred to as a rectangular area. When the number of rectangular areas is assumed to be i, the i-th rectangular area r_i on the projector coordinate system is defined as

$$r_i = \left\{(x,y) \;\middle|\; \left\lfloor \frac{x}{m} \right\rfloor = i \right\}. \tag{3}$$

We assume that a rectangular area r_i is projected on a rectangular area r'_i on the camera coordinate system. To match r_i and r'_i, we project the following light pattern $R(x,y)$ as a reference pattern that can divide the measurement space on the captured image into multiple rectangular areas:

$$R(x,y) = \left\lfloor \frac{x}{m} + 1 \right\rfloor \bmod 2. \tag{4}$$

$h(\xi,\eta)$ is defined as the number of switching obtained by counting the changes in brightness until pixel (ξ,η) in scanning $F(\xi,\eta)$ in the positive direction of ξ axis. $F(\xi,\eta)$ is the image captured when the reference light pattern $R(x,y)$ is projected. Thus, the region number at pixel (ξ,η) can be matched with that at $h(\xi,\eta)$, which can assign a rectangular area r'_i on the camera coordinate system as follows:

$$r'_i = \{(\xi,\eta) \mid h(\xi,\eta) = i\}. \tag{5}$$

In the mentioned below space encoding, we specify the number of the rectangle area i at a pixel (ξ,η) by using Eq. (5); and we then judge the type of gray code patterns that is projected on the pixel (ξ,η) at time t.

2) Selectable encoding types: Fig. 5 shows the types of gray pattern codes that are projected at a part of a certain line for eight frames when the light patterns defined by Eq. (1) and (2) are projected. Here the vertical axis represents time and the horizontal axis, the number of rectangular areas. In the figure, we show an example of spatio-temporal selection type encoding at a pixel (ξ,η); four bits are in the time direction and three bits are in the space direction, and they are referred for obtaining a space code value. Thus, we can obtain a space code value at a pixel (ξ,η) in a rectangular area i by using not only temporal encoding, or spatial encoding in a single direction but also spatio-temporal selection type encoding, which refers image information both temporally and spatially.

In this paper, we introduce n selectable space code values ${}^pX(\xi,\eta,t)$ on a pixel (ξ,η) at time t, whose number of referred bits in time and space except the specified pixel are $(n-1,0),(n-2,1),\cdots,(0,n-1)$, respectively. n is the number of bits of space codes. $p(=1,\cdots,n)$ is an alternative parameter for space coding such that the space encoding is close to the space pattern selection when p is small, while it is close to the temporal one when p is large.

Here, $g(\xi,\eta,t)$ is a binarized image obtained from a camera at time t, which corresponds to coded structured light patterns. We abbreviate the binarized image $g(\xi,\eta,t)$ that belongs to a rectangular area i as ${}^ig_t$, and the space code value ${}^pX(\xi,\eta,t)$ is also abbreviated as ${}^pX_t$.

Eq. (6)∼(13) are enumerated as examples of selectable space code values when $n=8$. Here, ${}^ig'_t = {}^ig'_t(\xi,\eta,t)$ is a value obtained by spatial neighborhood processing. ${}^ig'_t$ is set to 0 or 1, which is the greater value when the numbers of 0, 1 of the binarized image $g(\xi,\eta,t)$ are counted in the ξ direction for the nearest i-th rectangular area to a pixel (ξ,η).

$${}^1X_t = {}^ig_{t-4}\,{}^ig_{t-3}\,{}^ig_{t-2}\,{}^ig_{t-1}\,{}^ig_t\,{}^ig_{t-7}\,{}^ig_{t-6}\,{}^ig_{t-5} \tag{6}$$

$${}^2X_t = {}^ig_{t-4}\,{}^ig_{t-3}\,{}^ig_{t-2}\,{}^ig_{t-1}\,{}^ig_t\,{}^{i+1}g'_t\,{}^ig_{t-6}\,{}^ig_{t-5} \tag{7}$$

$${}^3X_t = {}^ig_{t-4}\,{}^ig_{t-3}\,{}^ig_{t-2}\,{}^ig_{t-1}\,{}^ig_t\,{}^{i+1}g'_t\,{}^{i+2}g'_t\,{}^ig_{t-5} \tag{8}$$

$${}^4X_t = {}^ig_{t-4}\,{}^ig_{t-3}\,{}^ig_{t-2}\,{}^ig_{t-1}\,{}^ig_t\,{}^{i+1}g'_t\,{}^{i+2}g'_t\,{}^{i+3}g'_t \tag{9}$$

$${}^5X_t = {}^{i-4}g'_t\,{}^ig_{t-3}\,{}^ig_{t-2}\,{}^ig_{t-1}\,{}^ig_t\,{}^{i+1}g'_t\,{}^{i+2}g'_t\,{}^{i+3}g'_t \tag{10}$$

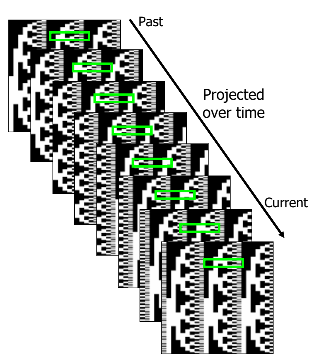

	2	3	4	5	6	7	0
2	3	4	5	6	7	0	1
3	4	5	6	7	0	1	2
4	5	6	7	0	1	2	3
5	6	7	0	1	2	3	4
6	7	0	1	2	3	4	5
7	0	1	2	3	4	5	6
0	1	2	3	4	5	6	7

Fig. 5. Spatio-temporal selection type encoding $(p=4)$

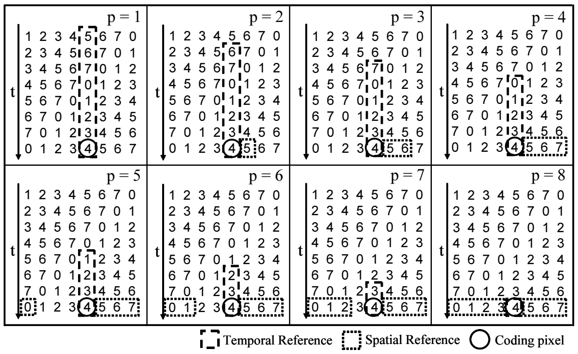

Fig. 6. Types of encoding

$$^{6}X_t = {}^{i-4}g'_t\,{}^{i-3}g'_t\,{}^{i}g_{t-2}\,{}^{i}g_{t-1}\,{}^{i}g_t\,{}^{i+1}g'_t\,{}^{i+2}g'_t\,{}^{i+3}g'_t \qquad (11)$$

$$^{7}X_t = {}^{i-4}g'_t\,{}^{i-3}g'_t\,{}^{i-2}g'_t\,{}^{i}g_{t-1}\,{}^{i}g_t\,{}^{i+1}g'_t\,{}^{i+2}g'_t\,{}^{i+3}g'_t \qquad (12)$$

$$^{8}X_t = {}^{i-4}g'_t\,{}^{i-3}g'_t\,{}^{i-2}g'_t\,{}^{i-1}g'_t\,{}^{i}g_t\,{}^{i+1}g'_t\,{}^{i+2}g'_t\,{}^{i+3}g'_t \qquad (13)$$

Fig. 6 shows eight space encoding types defined by Eq. (6)∼(13). The example of Fig. 5 is a case of $p = 4$. Space encoding that refers only to information along the time axis ($p = 1$) is effective for measuring objects with no motion,

When $p = 8$, space encoding type refers only to information in a single projected image. The encoding type is effective in measuring the shapes of moving objects because its accuracy is independent of the motion of objects; however, a disadvantage is that measurement errors may increase when undulated shapes are measured.

3) Adaptive selection of encoding types: Next, we introduce a criterion for the adaptive selection of encoding types defined by Eq. (6)∼(13), which focuses on the brightness changes in space code images. The introduced criterion is based on the frame differencing feature, which is obtained by differentiating a space code image $T(\xi,\eta,t)$ at time t from a space code image $S(\xi,\eta,t-1)$ at time $t-1$. Here, $T(\xi,\eta,t)$ is the space code image that refers only to information along the time axis, and $S(\xi,\eta,t-1)$ is the space code image in a previous frame selected by the below-mentioned Eq. (15). After differentiating, the criterion is provided for every divided square image region whose unit is $s \times s$ pixels by calculating the summation of the differentiating result as follows:

$$D(\xi',\eta',t) = \sum_{(\xi,\eta)\in q(\xi',\eta')} T(\xi,\eta,t) \oplus S(\xi,\eta,t-1). \qquad (14)$$

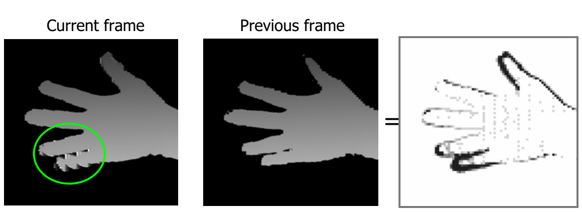

(a) Code image by temporal reference
(b) Code image by temporal-spatial reference
(c) An image that showed level of brightness change

Fig. 7. Criterion for spatio-temporal encoding

Here, the operator $\oplus$ shows an exclusive-OR operation, and $q(\xi',\eta')$ means the ξ'-th and η'-th $s \times s$ pixels block area in the ξ and η direction, respectively. $T(\xi,\eta,t_0)$ is initially set to $S(\xi,\eta,t_0-1)$ at time t_0, which is the start time to generate space codes. The criterion $D(\xi',\eta',t)$ corresponds to the number of pixels where the values of $T(\xi,\eta,t)$ are different from that of $S(\xi,\eta,t-1)$ in the block area $q(\xi',\eta')$.

The space code image $T(\xi,\eta,t)$ is not always encoded correctly in the measurement of moving objects because it refers to the only information along the time axis. Meanwhile, the space code image $S(\xi,\eta,t)$, which is generated by the spatio-temporal selection type encoding defined by Eq. (15), is robust to errors by the motion of measured objects. Based on the properties of the space code images, the criterion $D(\xi',\eta',t)$ is defined with a frame differencing calculation for every block area in order to detect the coding errors caused by motion.

Based on the criterion $D(\xi',\eta',t)$, the spatio-temporal encoding type $p = p(\xi',\eta',t)$ is selected from the encoding types ${}^{p}X_t$ defined by Eq. (6)∼(13) for every block area $q(\xi',\eta')$ at time t, subsequently a spatio-temporal selection type space code image $S(\xi,\eta,t)$ is obtained by using the calculated encoding types for all the block areas. In this paper, the spatio-temporal encoding type $p = p(\xi',\eta',t)$ is decided as follows:

$$p(\xi',\eta',t) = \begin{cases} n & (D(\xi',\eta',t) = s^2) \\ \left\lfloor \dfrac{nD(\xi',\eta',t)}{s^2} \right\rfloor + 1 & (\text{otherwise}) \end{cases} . \qquad (15)$$

Fig. 7 shows an example of our introduced criterion for spatio-temporal encoding in the case that a human opens and closes his fingers. In this figure, (a) space code image $T(\xi,\eta,t)$ by temporal reference, (b) space code image $S(\xi,\eta,t-1)$ by temporal-spatial reference in a previous frame, and (c) selected spatial encoding types $p(\xi',\eta',t)$, are shown. Here, the value of p increases when the tone becomes darker, as shown in Fig. 7(c).

It can been seen that in the area where code errors are caused by the motion of fingers p increases; in other words, space codes that are robust to motion are selected. Meanwhile, in the area where motion is slight, p decreases; in other words, space codes that enable accurate shape measurement for the static scenes, are selected. Thus, we can select spatio-temporal encode types adaptively according to the defined criteria based on frame differencing features.

4) Calculation of three-dimensional information: In order to calculate three-dimensional information from the space code image $S(\xi,\eta,t)$, $S(\xi,\eta,t)$ is required to transform based on the relationship between the location of a camera and a projector, as was the case in the previously-reported coded structured light pattern projection methods. In this paper, we transform the space code image into the three-dimensional information at each pixel using a method described in reference [4].

The three-dimensional coordinate $\mathbf{X}(t)$ is obtained from the pixel position (ξ,η) on the camera, and its space code value $S(\xi,\eta,t)$ is obtained by solving the following simultaneous equation with a 3×4 camera transform matrix

$\mathbf{C}$ and a 3×4 matrix $\mathbf{P}$,

$$H_c \begin{bmatrix} \xi \\ \eta \\ 1 \end{bmatrix} = \mathbf{C} \begin{bmatrix} \mathbf{X}(t) \\ 1 \end{bmatrix}, \tag{16}$$

$$H_p \begin{bmatrix} S(\xi, \eta, t) \\ 1 \end{bmatrix} = \mathbf{P} \begin{bmatrix} \mathbf{X}(t) \\ 1 \end{bmatrix}. \tag{17}$$

Here, H_c and H_p are parameters, and the camera transform matrix $\mathbf{C}$ and the projector matrix $\mathbf{P}$ must be obtained by prior calibration. By transforming all the pixels in the image using Eq. (16) and (17), a three-dimensional image is obtained as the result of our introduced coded structured light pattern projection method.

IV. Experiment

A. Experimental system

To verify our proposed method, off-line experiments for three-dimensional shape measurement are carried out on an experimental system; here, an off-line high-speed video camera and a high-speed DLP projector operate simultaneously.

Fig. 8 and Fig. 9 show its located configuration and its overview, respectively. The off-line high-speed video camera is FASTCAM-1024PCI (Photron Ltd.) can capture a 1024 × 1024 pixels 10 bit image at 1000 fps. The high-speed DLP projector comprises DMD (Digital Micromirror Device) Discovery 1100 (Texas Instruments Ltd.), ALP (Accessory Light modulator Package) controller, and LED Integrated Optical Module (ViALUX GmbH). The projector can project a 1024 × 768 pixels binary image at a frame rate of 1000 fps or more.

The distance between the camera and projector is approximately 18 cm, and a background screen is placed at a distance of approximately 110 cm from them. In this case, light patterns from the projector are projected over an area of 37 cm × 37 cm on the screen. Here the camera is properly set such that the rectangular areas defined in Section III-C.1 in the x direction is not distored even if the height of measured objects changes.

In the experiments, a light pattern of 768 × 768 pixels defined by Eq. (1) is projected at 1000 fps, and the number of bits of space codes and the width of rectangular areas are set to $n = 8$ and $m = 4$, respectively. The high-speed video camera captures a 1024 × 1024 pixels 10 bit image at 1000 fps so that the projected light patterns are settled in the captured image. Here, the projector and the camera are synchronized electrically for frame correspondence. In order to reduce errors caused by illumination or surface properties, a binary image for space encoding is binarized by differencing a pair of positive and negative projection images, which are generated by projecting a consecutive pair of light patterns whose black and white are reversed. The size of the block area is set to 8 × 8 pixels ($s = 8$) to calculate the criterion for the selection of encoding types.

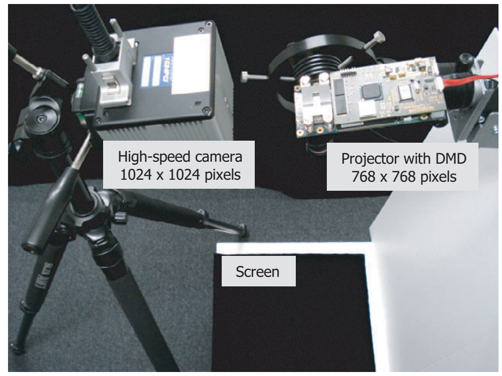

Fig. 9. Overview of experimental system

B. Experimental results

To evaluate our proposed algorithm, we experiment with three types of moving objects and observe the temporal changes in their three-dimensional shapes.

First, we show the measured result for a rotating plane object in Fig. 10. The figures on the left are the images captured by a video camera with a frame rate of 30 fps; the

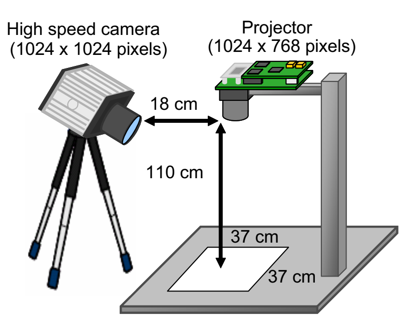

Fig. 8. Configuration of experimental system

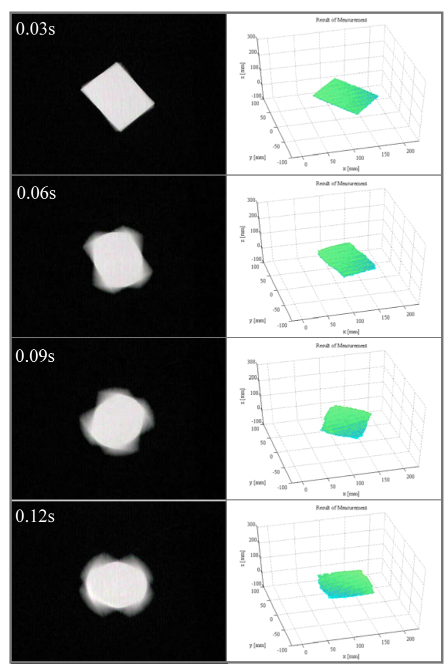

Fig. 10. Experimental result for a rotating plane

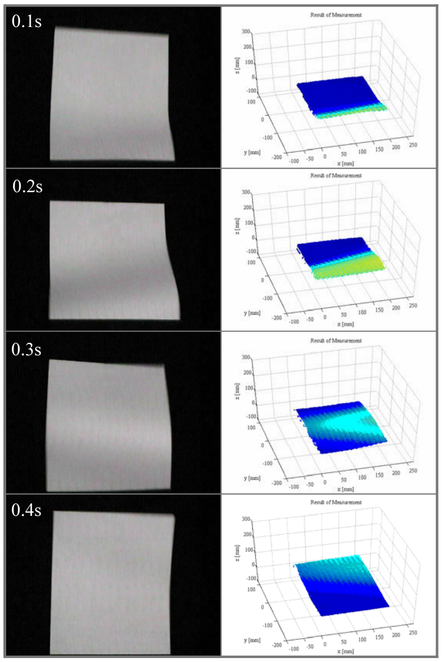

Fig. 11. Experimental result for a waving paper

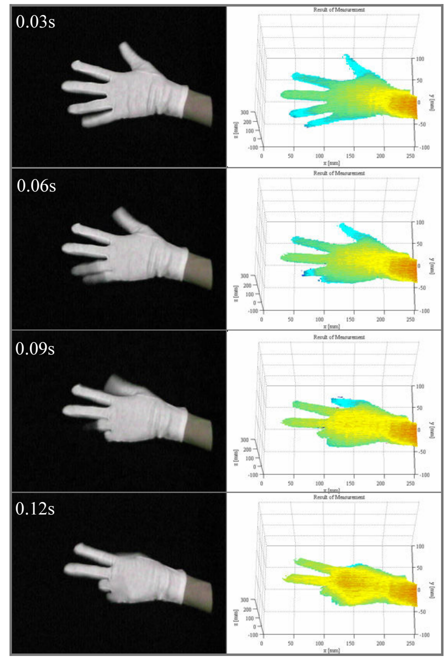

Fig. 12. Experimental result for a moving hand

figures on the right are three-dimensional images calculated by our proposed method, and their interval is set to 0.03 s in the figure. Here, we have also confirmed the acquisition of three-dimensional shapes at a frame rate of 500 fps. The measured object is a 8.5 cm $\times$ 10.0 cm plane, which is rotated at approximately 5.5 rotations per second by a DC motor. It can be seen that three-dimensional shape information can be acquired even if the measured object moves quickly.

Next, we show the measured three-dimensional shape for a waving paper in Fig. 11, whose interval is 0.1 s. Here, the measured object is a A4 paper (297 mm $\times$ 210 mm), which is waved in the vertical direction. From the figure, it can be seen that the temporal changes in the three-dimensional shape, which are generated by wave propagation, become visible.

Finally, we show the measured three-dimensional shape of a human hand whose fingers move quickly in Fig. 12; the interval is 0.03 s. Here the time required by a human to change his fingers' shape from "scissors" to "paper" is approximately 0.1 s or more. It can be seen that we can acquire the three-dimensional shape of an object that has a complicated shape, such as a human hand; further, quick movments of the fingers or changes in the height of the back of the hand can also be detected in the form of three-dimensional shape.

V. Conclusion

In this paper, we propose a spatio-temporal selection type coded structured light projection method for the acquisition of three-dimensional images at a high-speed frame rate, which can select adaptive space encoding types according to the temporal changes in the coded images. We also built a verification system that is composed of a high-speed projector and a high-speed video camera, and we evaluated the effectiveness of our proposed method by showing the results of three-dimensional shape measurement for various objects moving quickly at a high-speed frame rate such as 1000 fps.

References

[1] S. Yoshimura, T. Sugiyama, K. Yonemoto and K. Ueda. A 48kframes/s CMOS image sensor for real-time 3-D sensing and motion detection, in *ISSCC Tech. Dig.*, 2001, pp.94–95.

[2] Y. Oike, M. Ikeda and K. Asada. A CMOS image sensor for high-speed active range finding using column-parallel time domain ADC and position encoder, *IEEE Trans. Electron Devices*, vol.50, no.1, pp.152–158, 2003.

[3] J.L. Posdamer, M.D. Altschuler. Surface measurement by space-encoded projected beam systems, *Comput. Gr. Image Process.*, vol.18, no.1, pp.1–17, 1982.

[4] S. Inokuchi, K. Sato and F. Matsuda. Range imaging system for 3-D object recognition, in *Proc. Int. Conf. Patt. Recog.*, 1984, pp.806–808.

[5] D. Bergmann. New approach for automatic surface reconstruction with coded light, *Proc. SPIE*, vol.2572, pp.2–9, 1995.

[6] D. Caspi, N. Kiryati and J. Shamir. Range imaging with adaptive color structured light, *IEEE Trans. Pattern Anal. Mach. Intell.*, vol.20, no.5, pp.470–480, 1998.

[7] M. Maruyama, S. Abe. Range sensing by projecting multiple slits with random cuts, *IEEE Trans. Pattern Anal. Mach. Intell.*, vol.15, no.6, pp.647–651, 1993

[8] N.G. Durdle, J. Thayyoor and V.J. Raso, An improved structured light technique for surface reconstruction of the human trunk, in *Proc. Can. Conf. Elect. Comput. Eng.*, 1998, pp.874–877.

[9] L. Zhang, B. Curless and S.M. Seitz. Rapid shape acquisition using color structured light and multi-pass dynamic programming, in *Proc. IEEE Int. Symp. 3D Data Processing Visualization and Transmission*, 2002, pp.24–36.

[10] J. Salvi, J. Batlle and E. Mouaddib. A robust-coded pattern projection for dynamic 3d scene measurement, *Int. J. Patt. Recog. Lett.*, vol.19, pp.1055–1065, 1998.